

# ANALYTICAL AND EXPERIMENTAL MOTION ANALYSIS OF FINGER FOLLOWER TYPE CAM-VALVE SYSTEM WITH A HYDRAULIC TAPPET

Won-Jin Kim\*, Hyuck-Soo Jeon\* and Youn-Sik Park\*

(Received September 11, 1989)

In this paper, the motion of a finger-follower type cam valve system with a hydraulic tappet was analytically and experimentally studied. First, the exact contact point between cam and follower for each corresponding cam angle was searched by kinematic analysis. Then a 6 degree of freedom lumped spring-damper-mass model was constructed to simulate the valve motion analytically. When constructing the model, most of the parameters were experimentally determined. But several values which are difficult to derive experimentally such as damping coefficients were determined with engineering intuition. In order to show the effectiveness of the analytical model, the predicted cam-valve motion was directly compared with the measured valve and tappet motions.

**Key Words :** Finger-Follower (Oscillating Roller Follower), Overhead Cam(OHC), Cam-Valve System, Jump, Bounce

## NOMENCLATURE

$A_e$  : Equivalent cross-sectional area of oil chamber in tappet,  $m^2$   
 $C_{s1}, C_{s2}, C_{s3}$  : Equivalent damping coefficients of valve spring, N/m  
 $C_{se}$  : Damping coefficient of valve seat, N-s/m  
 $C_{tj}, C_{vj}, C_{jc}$  : Equivalent damping coefficients of contact point, N-s/m  
 $C_{tp}$  : Equivalent damping coefficient of tappet, N-s/m  
 $f_0$  : Fundamental natural frequency of valve spring, Hz  
 $F_0$  : Initial compression force of valve spring, N  
 $F_{tj}, F_{vj}, F_{jc}$  : Contact forces at each contact point, N  
 $F_{tj0}, F_{vj0}, F_{jc0}$  : Initial contact forces at each contact point, N  
 $h$  : Clearance between cylinder and plunger, mm  
 $H_e$  : Length of compressed oil chamber, mm  
 $I_f$  : Follower moment of inertia,  $kg-m^2$   
 $K_0$  : Valve spring stiffness, N/m  
 $K_e$  : Equivalent stiffness of tappet oil chamber, N/m  
 $K_{s1}, K_{s2}, K_{s3}$  : Equivalent stiffness coefficients of valve spring, N/m  
 $K_s$  : Stiffness of tappet soft spring, N/m  
 $K_{tj}, K_{vj}, K_{jc}$  : Equivalent stiffness coefficients of contact point, N/m  
 $L$  : Plunger length, mm  
 $L_{tj}$  : Lever arm of force  $F_{tj}$ , mm  
 $L_{vj}$  : Lever arm of force  $F_{vj}$ , mm  
 $m_c$  : Mass of oil inside tappet oil chamber, kg  
 $M_f$  : Follower mass, kg  
 $M_t$  : Equivalent tappet mass, kg  
 $M_v$  : Equivalent valve mass, kg

$m_1, m_2$  : Equivalent valve spring masses, kg  
 $R_p$  : Radius of tappet plunger, mm  
 $R_c$  : Radius of cam base circle, mm  
 $R_{ab}$  : Distance from cam pivot to follower pivot, mm  
 $R_l$  : length of oscillating roller follower, mm  
 $R_f$  : Radius of roller in roller follower model, mm  
 $Y_f$  : Follower displacement, mm  
 $Y_t$  : Tappet displacement,  $\mu m$   
 $Y_c$  : Cam lift, mm  
 $Y_v$  : Valve displacement, mm  
 $Y_{s1}, Y_{s2}$  : Displacements of equivalent valve spring masses, mm  
 $\theta_f$  : Angular rotation of follower, radian  
 $\mu$  : Oil viscosity coefficient, Pa-s  
 $E$  : Bulk modulus,  $N/m^2$   
 $\theta$  : Angular rotation of cam, radian

## 1. INTRODUCTION

When designing a cam-valve train of internal combustion engine, there are many things to be considered such as valve lift area, peak cam acceleration, proper cam event angle, ramp velocity, etc. As increasing the operation speed of internal combustion engine, the dynamic effect of cam-valve system becomes more important. Recently, some researches have been done focusing the dynamic effects on cam-valve system. Akiba, et al.(1981) constructed a 4 degree of freedom model to analyze an OHV (Overhead Valve) type cam-valve system and studied the dynamic effects on the system motion. Jeon and Park(1989) tried to analyze the same type of valve system with a lumped mass dynamic model and designed an optimal cam shape considering dynamic effects. Pisano and Freudenstein (1982) developed a dynamic model of a high speed valve system capable of predicting both normal system response as well as pathological behavior associated with onset of jumping, bounce, and spring surge. Previous researches in high-speed cam system had been almost focused on systems with a constant rocker-arm ratio and on the valve

\*Department of Mechanical Engineering, Korea Advanced Institute of Science and Technology, P.O.Box 150 Cheongruang, Seoul 130-650, Koera

train separation phenomena. Especially, the analysis for cam system having a hydraulic tappet has not been thoroughly studied.

In this work, an OHC cam-valve train with a hydraulic tappet and a finger follower, was analyzed analytically with lumped mass model and its reliability was verified experimentally. The cam-follower system used in this work is characterized with its complex dynamics of hydraulic tappet and the nonlinearity from varying rocker-arm ratio. The rocker-arm ratio deviates as much as 34 percent from a baseline value of 1.47 as the contact point between cam and follower moves. The pivot end of the oscillating follower is supported not at a fixed point but at a vertically moving pivot mounted at top a hydraulic tappet. The major role of the hydraulic tappet is to remove the valve lash which gives harmful impact within valve train. But in high operating speed region, the hydraulic tappet can be operated abnormally and can make an unusual valve train motion. Therefore, the characteristics of the hydraulic tappet must be considered in valve train dynamic model. The primary research for a similar cam system was done by Chan and Pisano (1987). They established six degrees of freedom model considered translational and rotational motion of oscillating follower and valve. But they used a simple single degree of freedom model for the hydraulic tappet. They focused only on analytical work and did not attempt to verify the results experimentally

## 2. VALVE TRAIN MODELING

The actual overall shape of an OHC type cam-valve train is shown in Fig.1. In order to describe the valve motion precisely, the valve train was modeled with 6 degree of freedom. Those are valve opening and closing motion,  $Y_v$ , hydraulic tappet translational motion,  $Y_t$ , finger-follower translational and rotational motion,  $Y_f$  and  $\theta_f$ , and two additional degree of freedom  $Y_{s1}$  and  $Y_{s2}$ , which represent valve spring translational motion. The reason for taking valve spring motions  $Y_{s1}$  and  $Y_{s2}$  is to consider valve spring surge phenomenon. It is known that valve spring surge affects

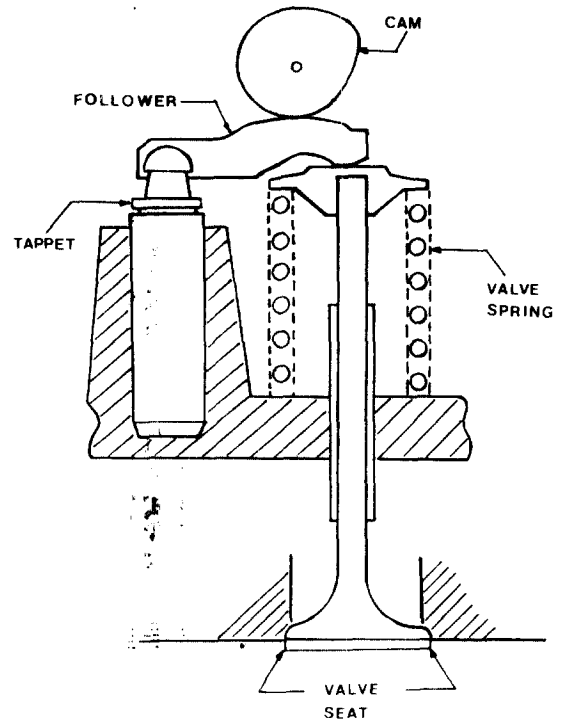


Fig. 1 Schematic of finger follower valve train

greatly on valve motion especially when the operation speed is high. Because camshaft can be considered as rigid and fixed on its bearing, its dynamic characteristics was neglected in the model.

All the components and the contact points of the cam-valve system were modeled with equivalent mass, springs and dampers as shown in Fig. 2. The details of modeling procedure are explained as follows.

### 2.1 Contact Point Modeling

As shown in Fig. 1 the finger-follower type cam-valve train

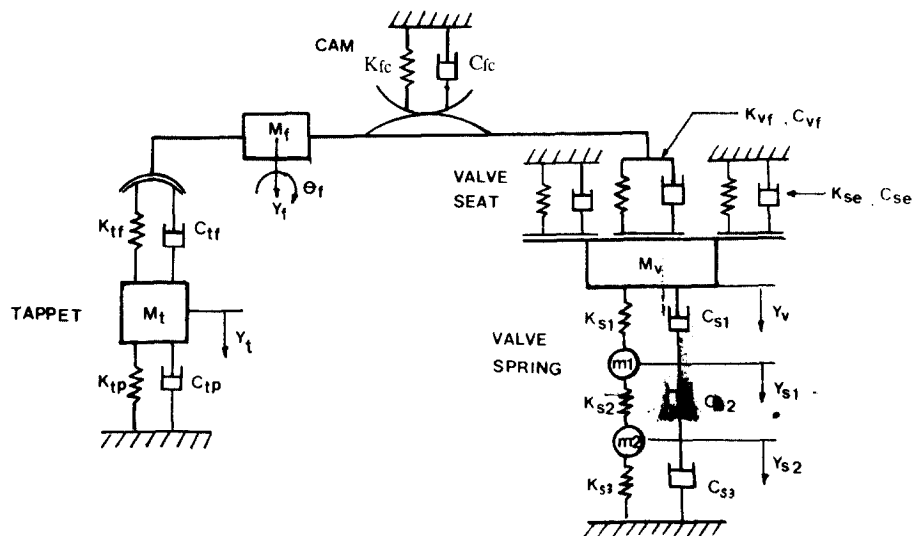


Fig. 2 Used model

has 4 contact points between valve train components. Those are between follower and tappet, follower and cam, follower and valve, and valve seat and valve. The contact at valve seat occurs periodically as different with others which should maintain continuous contact. The equivalent valve seat stiffness ( $K_{se}$ ) and damping ( $C_{se}$ ) coefficients were taken from the previously published literature (Chan and Pisano, 1987). On the other hand, the equivalent damping and stiffness coefficients at other contact points were predicted by Hertz contact theory utilizing shape factor, modulus of elasticity, and Poisson's ratio. As assuming the proper range of contact forces, the corresponding contact stiffness was calculated by Hertz contact theory. Then the equivalent stiffnesses at each contact point were determined by least square error curve fit from obtained contact stiffnesses (Roark and Young, 1976). It was assumed that the contact between tappet and follower is an internal contact of two spheres, between cam and follower is a contact of two cylinders, and between follower and valve is a contact of a cylinder on a plane.

The damping coefficients at each contact point were assumed as 0.06 and the critical damping coefficient ( $C_{cr}$ ) can be calculated using Eq.(1). Where  $M_1$  and  $M_2$  are the equivalent masses of each contacting component. It was assumed that the equivalent masses of each contacting component ( $M_1$  and  $M_2$ ) are connected by a spring and a damper.

$$C_{cr} = 2\sqrt{\frac{KM_1M_2}{M_1+M_2}} \quad (1)$$

The equivalent mass ( $M_e$ ) of finger follower at each contact point can be obtained from Eq. (2) as considering the follower moment of inertia ( $I_f$ ).

$$M_e = \frac{M_f}{1 + (M_f l^2) / I_f} \quad (2)$$

where  $M_f$  is the follower equivalent mass and  $l$  is the distance between follower mass center and each corresponding contact point. The equivalent mass of camshaft at contact point is estimated to infinity as assuming that it is rigid and

fixed on its bearing. The equivalent masses of tappet and valve at other contact points are  $M_t$  and  $M_v$ .

## 2.2 Valve Spring Modeling

In order to consider valve spring surge effect, the valve spring was modeled with 2 masses ( $m_1$  and  $m_2$ ), 3 springs ( $K_{s1}$ ,  $K_{s2}$  and  $K_{s3}$ ), and 3 dampers ( $C_{s1}$ ,  $C_{s2}$  and  $C_{s3}$ ) with 2 degree of freedom ( $Y_{s1}$  and  $Y_{s2}$ ). Several assumptions were made in the valve spring modeling. Those are; (i) symmetry ( $K_{s1} = K_{s3}$  and  $C_{s1} = C_{s3}$ ), (ii) equivalency of static stiffness and fundamental natural frequency between model and fundamental natural frequency between model and actual system, (iii) proper damping assumption.

As considering that valve spring is in clamped-clamped boundary condition, the secondary natural frequency of valve spring becomes twice of the fundamental spring natural frequency. All the above assumptions give

$$\begin{aligned} m_1 = m_2 &= \frac{2}{3} K_0 / (\pi f_0)^2 \\ K_{s1} = K_{s3} &= \frac{8}{3} K_0, \quad K_{s2} = 4K_0 \end{aligned} \quad (3)$$

The spring rate and fundamental natural frequency of used valve spring are 35 KN/m and 504.46Hz, respectively. The damping is assumed as 4% proportional viscous damping.

## 2.3 Hydraulic Tappet Modeling

The left side of Fig. 3 shows the cross section shape of hydraulic tappet. Oil enters through entrance and fills the central cavity of tappet plunger. As the plunger moves down, the check valve is closed and the oil flows from oil chamber through narrow clearance between plunger and cylinder and generates damping force. In next step, when the plunger moves upward due to the spring positioned inside of oil chamber, the check valve is opened and oil is refilled in oil chamber. The hydraulic tappet was simplified as shown in the right side of Fig.3 and the equivalent stiffness of the tappet was estimated by assuming that the fluid is totally compressive and there is no flow through diametral clearance. The

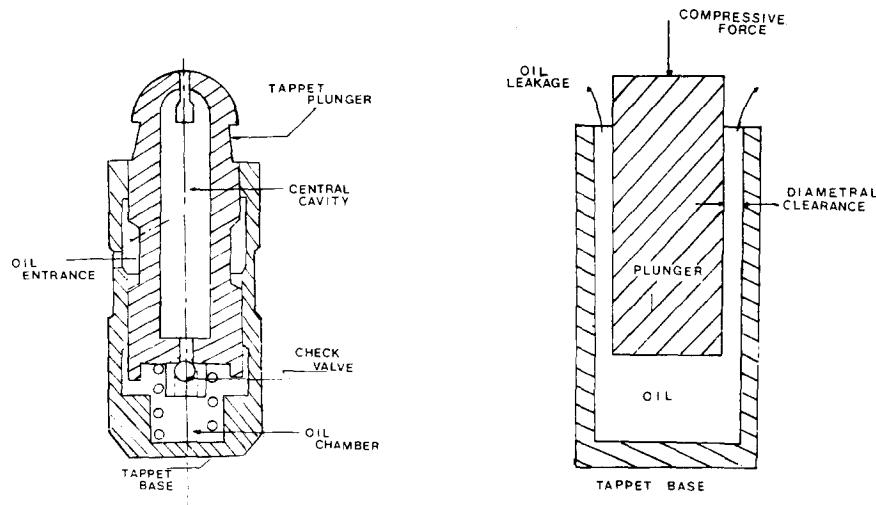


Fig. 3 Hydraulic tappet and its simplified operation drawing.

**Table 1** Tappet dimensions and properties

Parameter	Value
$A_e$	$1.213 \times 10^{-4} \text{m}^2$
$H_e$	10.15mm
$E$	$1.375 \times 10^9 \text{N/m}^2$
$\mu$	0.015Pa-s
$R_p$	7.9325mm
$h$	0.009mm
$L$	13.58mm

**Table 2** Used model parameters

\*stiffness of plunger spring

Mass(kg), (kg-m <sup>2</sup> )		Stiffness(N/m)		Damping(N-s/m)	
$M_t$	0.04567	$K_{tp}$	$6.648 \times 10^7$	$C_{tp}$	$2.635 \times 10^6 (\dot{Y}_t > 0)$
$M_f$	0.05981	$K_s^*$	$5.92 \times 10^9$		$1.128 (\dot{Y}_t < 0)$
$I_f$	$1.1527 \times 10^{-5}$	$K_{tf}$	$5.52 \times 10^7$	$C_{tf}$	118.97
$M_v$	0.08544	$K_{fc}$	$8.37 \times 10^7$	$C_{fc}$	197.97
$m_1$	0.0092	$K_{vf}$	$4.33 \times 10^7$	$C_{vf}$	94.13
$m^2$	0.0092	$K_{se}$	$1.31 \times 10^7$	$C_{se}$	634.77
		$K_{s1}, K_{s3}$	$9.33 \times 10^4$	$C_{s1}, C_{s3}$	2.355
		$K_{s2}$	$1.40 \times 10^5$	$C_{s2}$	3.534

relationship is

$$K_e \approx \frac{A_e E}{H_e} \quad (4)$$

where  $E$  is bulk modulus,  $H_e$  is the length of compressed oil chamber, and  $A_e$  is plunger area.

On the other hand, the equivalent damping coefficient was estimated by assuming that the oil is totally incompressible. It was assumed that the excessive oil due to plunger motion flows completely through the diametral clearance. Then the equivalent damping value can be predicted from the theory of fluid mechanics. It is known that the damping coefficient changes with the direction of plunger motion. Those are

$$C_d = \frac{6\mu\pi L R_p^2 (R_p + h)}{h^3} + \frac{2\mu\pi R_p L (3R_p + 4h)}{h^2} \quad \text{if } \dot{Y}_t > 0 \quad (5)$$

$$C_d = \frac{2\mu\pi L R_p}{h} \quad \text{if } \dot{Y}_t < 0$$

where  $\mu$  is oil viscous coefficient,  $L$  is plunger length,  $R_p$  is plunger radius, and  $h$  is clearance between cylinder and plunger. All tappet dimensions and properties are given in Table 1.

Equations (4, 5) derived above are two extreme cases, one is assumed totally compressive and the other is totally incompressible. But in actual situation, the drag force ( $F_d$ ) due to plunger motion will be placed somewhere in the middle of the two values (Kreuter and Mass, 1987). As introducing two coefficients  $\alpha$  and  $\beta$  ( $0 < \alpha < 1, 0 < \beta < 1$ ), the drag force can be modeled as Eq.(6).

$$F_d = \alpha C_d \dot{Y}_t + \beta K_e Y_t \quad (6)$$

where  $\alpha$  and  $\beta$  can be determined by comparing model simulation result with experimentally measured record.

#### 2.4 Mass and Moment of Inertia Modeling

Valve, tappet plunger, and follower mass ( $M_v$ ,  $M_t$ , and  $M_f$ ) were directly measured. The follower moment of inertia ( $I_f$ )

was carefully calculated considering its geometrical shape. All the used mass, stiffness and damping values were summarized in Table 2.

### 3. ANALYSIS

The finger-follower type OHC cam-valve system is characterized with varying rocker-arm ratio with cam shaft rotations. So the kinematical analysis to search the exact contact points between cam and follower is inevitable before doing dynamic analysis.

#### 3.1 Kinematical Analysis

When searching the point where cam and follower contacts, the tappet was considered fixed point, It was found that the influence of tappet motion upon contact point is negligible. The tappet motion, which is at most 0.1(mm), is enough small and can be considered negligible and differs in order of magnitude with cam lift. When the cam data is given with desired cam lift ( $S$ ), the actual cam shape ( $X, Y$ ), contacting with a flat follower, can be obtained from Eq.(7) The baseline rocker-arm ratio is 1.47 and the fluctuating range of rocker-arm ratio varies from 1.15 to 1.97 during the cycle.

$$\begin{aligned} X &= (R_c + S) \cos\theta - \frac{dS}{d\theta} \sin\theta \\ Y &= (R_c + S) \sin\theta + \frac{dS}{d\theta} \cos\theta \end{aligned} \quad (7)$$

where  $R_c$  is cam base circle,  $\theta$  is cam angle,  $S$  is flat follower displacement, and  $X$  and  $Y$  specify cam shape. The increment of  $S$  about  $\theta$  can be calculated with cubic spline interpolation (Shoup, 1979). When the cam shape ( $X, Y$ ) is given, the contact point between cam and follower can be found by kinematical analysis. Fig. 4 shows the idea how to find the contact point. The procedures are, first, rotate the follower around a fixed cam, then find out the locus of follower center ( $CC'$ ) Next, search the contact point for each follower rotating angle ( $\theta_c$ ) using the principle that the contact point is

the point where the line connecting cam center ( $A$ ) and the follower center (any point in locus  $CC'$ ) crosses with the tangent line at the corresponding cam angle. Then the contact point locus can be determined by rotating the searched contact point to the backward as much as the corresponding cam angle ( $\theta_c$ ). The kinematic dimensions of Fig. 4 are given in Table 3. The instantaneous rocker-arm ratio is calculated by dividing the total length of the finger-follower with the horizontal distance between the pivot point and cam and follower contact point for each corresponding cam angle. The obtained contact point locus and the corresponding fluctuating rocker-arm ratio for this study are shown in Fig. 5 (a),(b).

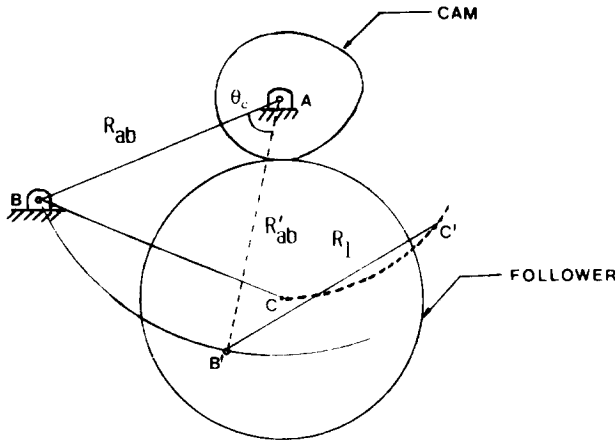


Fig. 4 Kinematic analysis of roller follower.

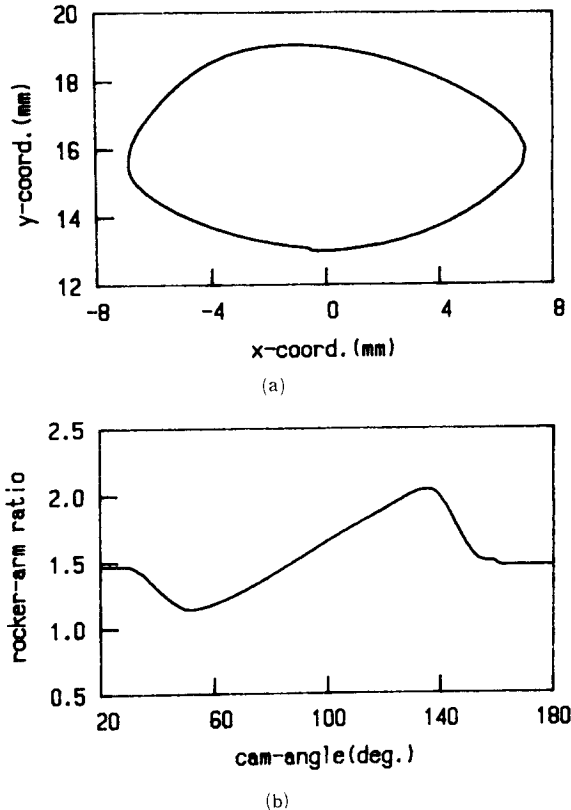


Fig. 5 Contact point locus and fluctuating rocker arm ratio

### 3.2 Dynamical Analysis

When the cam shape, operation speed and follower shape are given, the equations of motion can be easily constructed. During the calculation of contact point, all dimensions of  $L_{fc}$  (distance between tappet and follower mass center),  $L_{vf}$  (distance between cam contact point and follower mass center), and  $L_{vf}$  (distance between valve and follower mass center) can be obtained. Here,  $L_{tf}$  and  $L_{vf}$  given in Table 3 are constant.  $L_{fc}$  is calculated with instantaneous contact point. The effect of the fluctuating rocker-arm ratio on the valve train dynamics is represented by varying  $L_{fc}$ . Then the equations of motion can be constructed as

$$\begin{aligned}
 M_t \ddot{Y}_t &= F_{tf} - K_{tp} Y_t - C_{tp} \dot{Y}_t \\
 M_f \ddot{Y}_f &= F_{fc} - F_{tf} - F_{vf} \\
 I_f \ddot{\theta}_f &= F_{tf} L_{tf} + F_{fc} L_{fc} - F_{vf} L_{vf} \\
 m_1 \ddot{Y}_{s1} &= K_{s1} (Y_v - Y_{s1}) + C_{s1} (\dot{Y}_v - \dot{Y}_{s1}) \\
 &\quad - K_{s2} (Y_{s1} - Y_{s2}) - C_{s2} (\dot{Y}_{s1} - \dot{Y}_{s2}) \\
 m_2 \ddot{Y}_{s2} &= K_{s2} (Y_{s1} - Y_{s2}) + C_{s2} (\dot{Y}_{s1} - \dot{Y}_{s2}) \\
 &\quad - K_{s1} Y_{s2} - C_{s1} \dot{Y}_{s2} \\
 m_v \ddot{Y}_v &= F_{vf} - K_{se} Y_v - C_{se} \dot{Y}_v - K_{s1} (Y_v - Y_{s1}) \\
 &\quad - C_{s1} (\dot{Y}_v - \dot{Y}_{s1}) \quad \text{if } Y_v < F_o / K_{se} \\
 m_v \ddot{Y}_v &= F_{vf} - F_o - K_{s1} (Y_v - Y_{s1}) \\
 &\quad - C_{s1} (\dot{Y}_v - \dot{Y}_{s1}) \quad \text{if } Y_v > F_o / K_{se}
 \end{aligned} \tag{8}$$

where  $F_o$  is the precompressed force of valve spring (in this study,  $F_o = 275[N]$ )

The contact forces  $F_{tf}$ ,  $F_{fc}$ , and  $F_{vf}$  can be determined as Eq.(9).

$$\begin{aligned}
 F_{tf} &= K_{tf} (Y_f - L_{tf} \sin \theta_f - Y_t) + C_{tf} (\dot{Y}_f - L_{tf} \dot{\theta}_f \cos \theta_f - \dot{Y}_t) \\
 F_{fc} &= K_{fc} (Y_c - Y_f - L_{fc} \sin \theta_f) \\
 &\quad + C_{fc} (\dot{Y}_c - \dot{Y}_f - L_{fc} \dot{\theta}_f \cos \theta_f - \dot{L}_{fc} \sin \theta_f) \\
 F_{vf} &= K_{vf} (Y_f - Y_v + L_{vf} \sin \theta_f) \\
 &\quad + C_{vf} (\dot{Y}_f - \dot{Y}_v + L_{vf} \dot{\theta}_f \cos \theta_f)
 \end{aligned} \tag{9}$$

As examining the Eqs.(8, 9), all the equations are coupled and nonlinear. So numerical integration method (in this study, Runge-Kutta Method) was used to get all the components motion. As calculating the equation of motion, the separation phenomenon within valve train, such as jumping, can be checked at every time instance. The separation can be detected by examining the contact forces. The criterion judging jumping phenomenon at each contact point is as follows,

Between tappet and follower :

$$Y_f - Y_t - L_{tf} \sin \theta_f < -F_{tfo} / K_{tf}$$

Between cam and follower :

$$Y_c - Y_f - L_{fc} \sin \theta_f < -F_{fco} / K_{fc}$$

Between valve and follower :

$$Y_f - Y_v + L_{vf} \sin \theta_f < -F_{vfo} / K_{vf} \tag{10}$$

where  $F_{tfo}$ ,  $F_{fco}$  and  $F_{vfo}$  are the initial contact forces at each contact point. While calculating cam valve motion, the separation criterion was tested at every time instance. When one of the above criterion is satisfied, then the contact force becomes zero and we can judge that separation occurs between the corresponding components.

Table 3 Kinematic dimensions unit : mm

			unit : mm
$R_{ab}$	36.40	$R_f$	34.00
$R_l$	31.67	$L_{tf}$	14.22
$R_c$	13.00	$L_{vf}$	22.53

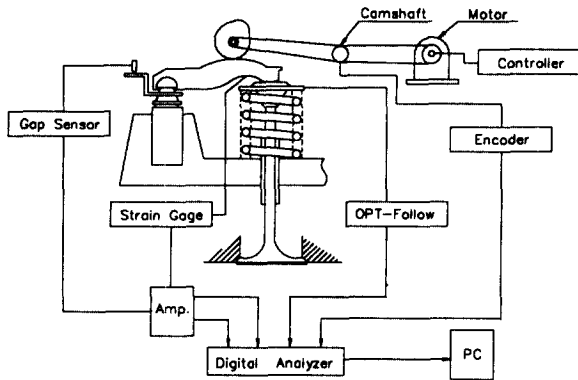


Fig. 6 Experimental apparatus

### 4. EXPERIMENT

In order to prove the effectiveness of the model simulation, experimental work was done and compared each other.

Figure 6. shows the experimental apparatus. While the OHC type cam-valve train was driven by a 100[kW] DC motor, valve displacement and hydraulic tappet motion were measured simultaneously. The valve displacement was measured with an opt-follow(noncontact type optical displacement measurement device), and the tappet motion was measured with a gap sensor. An encoder was placed at the one end of camshaft in order to average the measured signal. Special care was taken to eliminate problems caused by circulating engine oil. All the measurement were done as varying the camshaft running speed from 600 to 2450rpm.

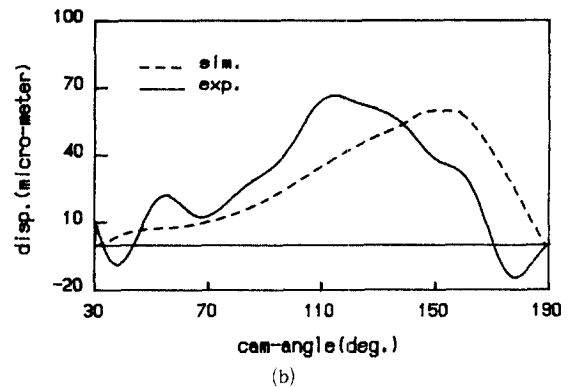
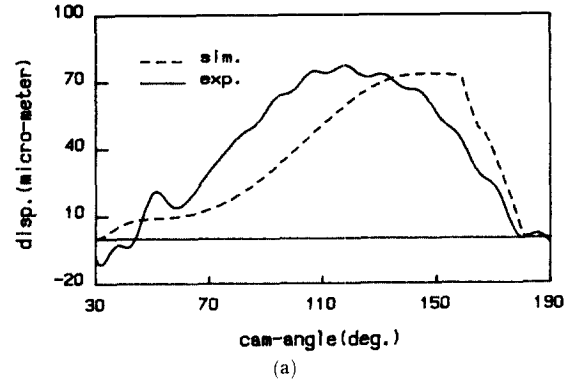
### 5. RUSULT AND DISCUSSION

Figure 7 compares the measured and simulated tappet leakage down at camshaft speed 900 and 1600 rpm. Figure 8 shows the measured maximum tappet leakage down. It is known that hydraulic tappet is stiffened as the speed of camshaft is increased. The maximum compression of the hydraulic tappet was about 100 μm at 800 rpm and approached a limit of about 60μm as the camshaft speed goes beyond 3000 rpm, as shown in Fig. 8. As explained before, the measured tappet motion was used to determine the weighting parameters  $\alpha$  and  $\beta$ , which determine the plunger drag force, by least square curve fit between the measurement and the analysis record. It was found that the weighting parameter varies with operation speed. For example,  $\alpha$  and  $\beta$  where 0.0071 and 0.28 when camshaft is driven by 900 rpm, but the values were changed to 0.0094 and 0.30 when the running speed was raised to 1600rpm.

Figures 9, 10, 11 show the measured and simulated valve displacements and velocities. The valve velocity was obtained by differentiating the measured valve displacement record.

Figure 9 compares the measured and analyzed valve motion when the camshaft was driven at 600rpm. It can be said that the model can simulate not only the peak valve displacement but also the cam event angle quite precisely.

Figure 10, 11 show the analysis and measurement when the camshaft speeds are 1600 rpm 2450rpm. As glancing at Figs.



(a) Camshaft speed 900 rpm  
(b) Camshaft speed 1600 rpm

Fig. 7 Tappet leakage down

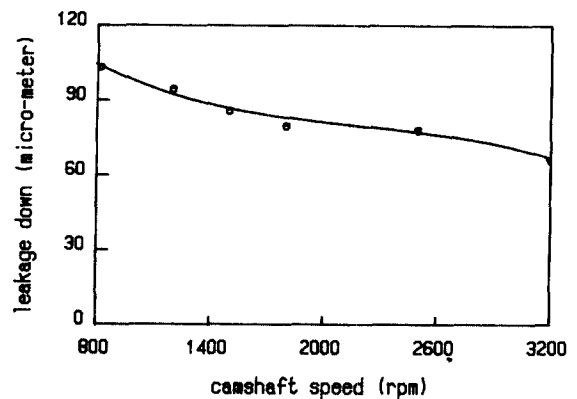


Fig. 8 Maximum tappet leakage down versus camshaft speed

9, 10, 11, we can conclude that the 6 degree of freedom lumped mass model used in this work is quite reliable to predict valve motion even in high operating speed.

Figure 12 shows a sample of contact forces at all contact points when the operation speed is 2450 rpm. It can be observed that the contact forces at the first peak position are reduced and at the second peak position are accentuated as compared with the value of constant rocker-arm ratio cam system due to fluctuating rocker-arm ratio. As examining the contact force record, we can easily predict the most possible area and corresponding cam angle where unwanted valve train separation can be occurred.

The experimentally verified model can be expanded not only to predict the maximum operation speed but also to

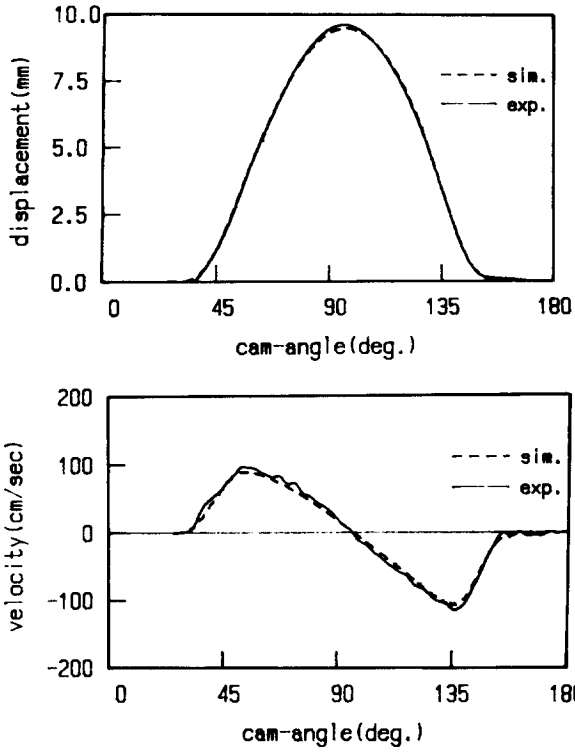


Fig. 9 Valve displacement and velocity(camshaft speed 600 rpm)

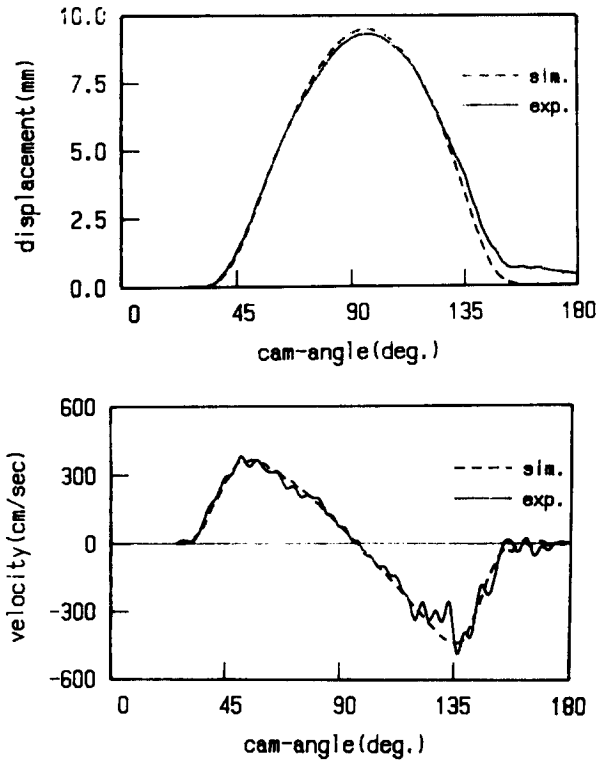


Fig. 11 Valve displacement and velocity (camshaft speed 2450 rpm)

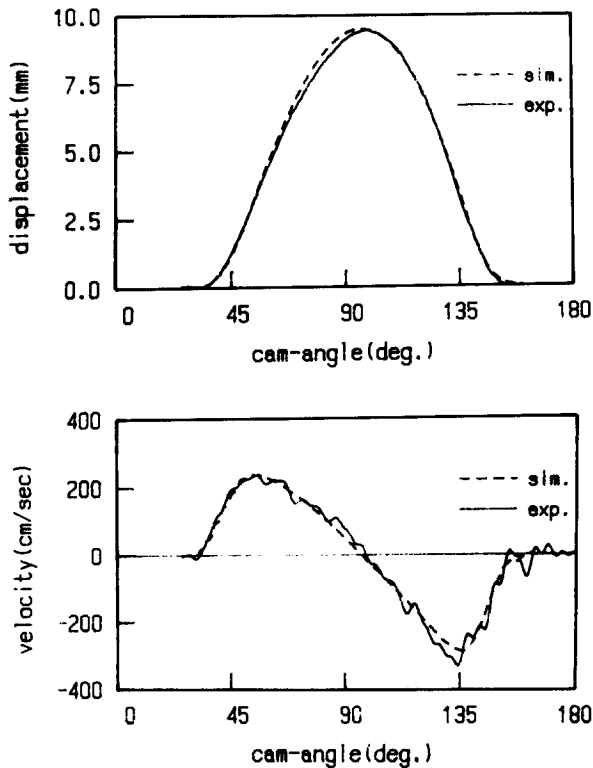
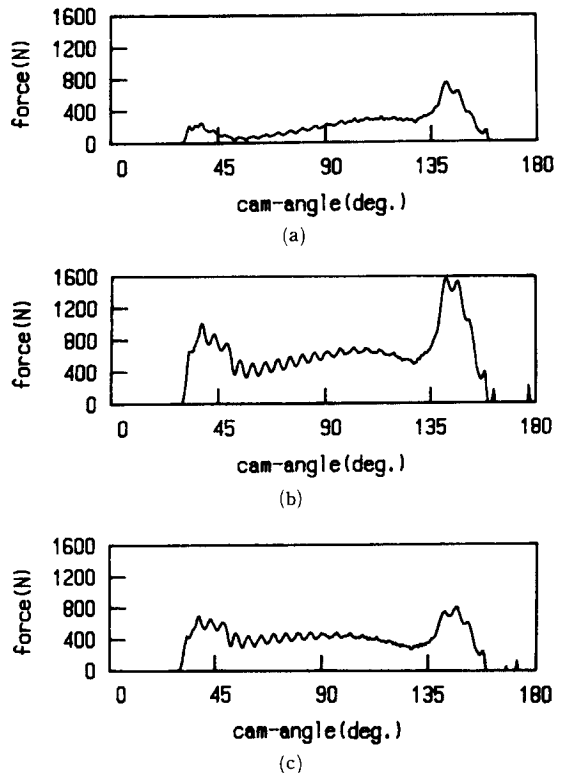


Fig. 10 Valve displacement and velocity (camshaft speed 1600 rpm)



(a) Between tappet and follower  
(b) Between cam and follower  
(c) Between valve and follower

Fig. 12 Contact forces for simulation (camshaft speed 2450 rpm)

optimize the valve train and cam shape.

## 6. CONCLUSIONS

In this work, a 6 degree of freedom lumped mass-spring-damper model was constructed and its effectiveness was experimentally verified. The varying rocker-arm ratio could be effectively included in dynamic model by kinematic analysis and its effect could be observed from simulation results of contact force. The hydraulic tappet model used for the pivot end of oscillating follower was constructed with the aids of experimental data. Consequently, it was found that the constructed numerical model is quite effective to predict finger-follower type OHC valve motion.

## ACKNOWLEDGMENT

This research was supported by Daewoo Motor Co. through a KAIST-Industry Consortium Project.

## REFERENCES

- Chan, C. and Pisano, A., 1987, "Dynamic Model of Fluctuating Rocker-Arm Ratio Cam System", ASME J. Mech. Trans. Automation in Design. Vol. 109. pp. 356~365.
- Jeon, H.S., Park, K.J. and Park, Y.S., 1989, "An Optimal Cam Profile Design Considering Dynamic Characteristics of Cam-Valve System," Experimental Mechanics, pp. 357~363.
- Kreuter, P. and Maas, G., 1987, "Influence of Hydraulic Valve Lash Adjusters on the Dynamic Behavior of Valve Trains", SAE Technical paper No. 870086.
- Pisano, A.P. and Freudenstein, F., 1982, "An Experimental and Analytical Investigation of Dynamic Response of a High-speed Cam-Follower System. Part 1 and Part2", ASME J.Mech. Trans. Automation in Design, Vol. 105, pp. 692~704.
- Roark, R. and Young, W., 1976, "Formulas for Stress and Strain", McGraw-Hill.
- Sakai, H. and Kosaki, H., 1976, "Analysis of Valve Motion in Overhead Valve Linkages-Roles of Valve Spring Surge in Valve Motion", Journal of the Faculty of Engineering, The University of Tokyo(B), Vol. 33, No.4 pp. 441~446.
- Akiba, K., Shimizu, A. and Sakai, H., "A Comprehensive Simulation of High Speed Driven Valve Trains", SAE Technical Paper No. 810865.
- Shoup, T., 1979. "A Practical Guide to Computer Methods for Engineers", Prentice-Hall.